Investigation of Chitosan Gelation Mechanisms by a Modeling Approach Coupled to Local Experimental Measurement

A. Venault
Dept. of Chemical Engineering, Chung Yuan Christian University, Chung-Li City, Taoyuan County 32023, Taiwan

R&D Center for Membrane Technology, Chung Yuan Christian University, Chung-Li City, Taoyuan County 32023, Taiwan

D. Bouyer and C. Pochat-Bohatier
UMR 5635 – CNRS, ENSCM, UM II, Institut Européen des Membranes, Place Eugène Bataillon, 34095 Montpellier Cedex 5, France

L. Vachoud
UMR Qualisud, UFR Sciences Pharmaceutiques et Biologiques, 34093 Montpellier Cedex 5, France

C. Faur
UMR 5635 – CNRS, ENSCM, UM II, Institut Européen des Membranes, Place Eugène Bataillon, 34095 Montpellier Cedex 5, France

DOI 10.1002/aic.12737
Published online August 8, 2011 in Wiley Online Library (wileyonlinelibrary.com).

The formation of chitosan hydrogels using experimental and modeling approaches are described. Chitosan gelation was induced by an ammonia intake from a liquid phase (wet process) or a gaseous phase (vapor process), involving three steps: (i) external mass transfer at the interface, (ii) internal transport within the polymer solution, and (iii) chemical reactions inducing gelation. The experimental study allowed quantifying gelation fronts speeds from local measurement. The main resistance to gelation was investigated for both gelation processes. Experimental results exhibited that internal diffusion through the chitosan matrix was the main resistance in the whole gelation mechanism. The numerical model involved a coupling between mass and heat transfer phenomena and chemical reactions, in transient conditions. Numerical results were first validated and then used as a predictive tool to investigate (i) coupled mechanisms localized in the chitosan matrix and (ii) the influence of operating conditions on gelation rates. © 2011 American Institute of Chemical Engineers *AIChE J,* 58: 2226–2240, 2012

Keywords: chitosan hydrogels, wet process, vapor process, mass transfers, modeling

Introduction

Chitosan is obtained from chitin, a natural biopolymer that can be found in the shells of crustaceans or in the exoskeleton of insects. The main difference between chitin and chitosan is the proportion of amino groups along the polymeric chains, characterized by the degree of acetylation (DA). Different values of DA lead to different physico-chemical properties and especially different solubilities. Hence, chitin is soluble in some organic solvents whereas chitosan is soluble in acid aqueous solutions.[1,2] Chitosan, under membrane or hydrogel form, has many interesting biological properties, making it suitable for the biomedical field, especially as a dressing for wounds caused by burns or bedsores.[3–6] In addition, it is very well tolerated by tissues and promotes their effective regeneration.

Correspondence concerning this article should be addressed to D. Bouyer at denis.bouyer@univ-montp2.fr.

As soon as the polymeric solution is exposed to a basic media, chitosan gelation occurs, involving three main mechanisms: (i) mass transport of the basic molecule (ammonia or sodium hydroxide for instance) to the chitosan solution surface; this step is mainly controlled by local hydrodynamics in the surrounding bulk solution; (ii) diffusion of the basic molecule through the polymeric system (from the top to the bottom); and (iii) chemical reaction between the basic molecule and the chitosan polymer chains, which are initially under protonated form and are deprotonated by the chemical reaction. The nature of the interface between the basic media and the polymeric solution can be either liquid/liquid or gas/liquid. In the first case, the process is the so called wet process.[7] In literature, the second process is often called the Vapor Induced Phase Separation (VIPS) process[8–11] for synthetic polymers. In this article, it is called the vapor gelation process since the gelation phenomenon cannot be assimilated to a phase separation induced by a change of the thermodynamic state.

In the last two decades, chitosan gelation has been investigated by classic experimental methods such as rheometric or

light scattering studies.[12,13] In a recent paper, another original method was investigated, permitting to follow global mass transfers during the vapor gelation process under perfectly controlled process conditions. In such conditions, dynamics of chitosan gelation could be followed and investigated. This experimental work was coupled to a modeling approach: the mass transfer was simulated before the gelation and numerical results were validated using experimental data collected in-line.[14]

The modeling approach has not been extensively reported in literature concerning the biopolymers systems, especially for chitosan or chitin system. To the best of our knowledge, only four previous studies have been published aiming at simulating natural polymer gelation by the vapor process.[14–17] Concerning the wet process, the modeling approach has never been described for chitosan nor chitin hydrogels yet. However, the modeling of polymeric membranes from synthetic polymers has been extensively reported in literature, when membranes are prepared by wet process[18–20] or by the VIPS process.[21–24] Concerning the wet process, Cheng et al. (1999) worked on poly(vinylidene fluoride) (PVDF) membrane formation and managed to predict with good accuracy the morphology of final matrices thanks to mass transfer modeling.[18] Later, Fernandes et al. (2001) presented a mathematical model that described the main features of phase inversion by immersion precipitation.[19] Their simulation was based on a planar geometry and Fickian diffusionnal approach, neglecting cross-diffusion terms in the expression of mass fluxes. It was able to reproduce both quantitatively and qualitatively experimental results regarding to morphological properties. At the same period, Kim et al. (2001) studied the formation of asymmetric membranes and the originality of their work was based on the setting up of mass transfer formalism at the interface.[20]

The mass transfer models concerning the VIPS process were developed later. The first one was proposed by Matsuyama et al. (1999).[21] Then, Khare et al. (2005) focused on the modeling of the phase separation for the quaternary system polyethersulfone/polyvinyl pyrrolidone/water/NMP.[22] Their model aimed at better understanding the asymmetric morphology obtained by VIPS process. Yip and McHugh (2006) proposed a model based on the Vrentas and Duda free-volume theory for four polymeric systems.[23] Recently, Bouyer et al. (2010) investigated (i) the influence of the diffusion formalism on the concentration profiles before phase separation and (ii) the influence of the formulation and the process parameters on the membrane morphology in the upper interface region for the poly(etherimide) (PEI)/1-methyl-2-pyrrolidone (NMP)/water system.[24]

Nevertheless, these modeling studies applied to thin films (membranes or hydrogels) were not validated using local data. In the best case, gravimetric measurements were conducted in-line and gave global data on the exchange rate between the polymeric system and the external environment. However, local measurements were never performed within the system to obtain local concentration gradients during the process. The global mass loss (or gain) rates classically used as the experimental validation depend on both the external and internal transfer phenomena. Thus, even if such global measurements are useful, they are not sufficient for validating complex mass transfer models, which often involve a coupling between mass and heat transfer phenomena. The numerical model proposed for the chitosan hydrogel fabrication must be considered with special attention since it involves not only a coupling between mass and heat transfers but also a coupling with chemical reactions involved in the gelation process (deprotonation reaction of the chitosan by the basic molecule). In such a case, the model is even more complex and the experimental procedure that must be developed to obtain local measurements during the gelation process must be improved to ensure a reliable validation.

The aim of this work is thus to develop such an experimental procedure to follow the formation of chitosan hydrogels, in wet and vapor gelation processes. Experimental data were obtained by a local measurement of the gelation front. Such an experiment has been conducted in-line and in-situ, and allowed highlighting the role of the coupled mechanisms involved in the gel formation (external transfer to the surface/internal transport within the polymeric solution/chemical reactions). In addition, the dynamics of the wet and vapor gelation processes will be compared. Such a study will also be helpful to propose a better validation of the numerical model, which will be developed in parallel for both the wet and vapor gelation processes. These models will be useful for predicting (i) the gelation time depending on the operating conditions and/or (ii) the expected morphological properties of the hydrogel. Finally, this article aims at extending the modeling approach to other geometries or other systems, to find out the optimal operating conditions to obtained chitosan hydrogels.

Methodology

Materials

Chitosan. Chitosan samples, produced from shrimp shell wastes, batch no 111, 112, and 342, were supplied by France Chitine (France). To determine the degree of acetylation of samples, chitosan powder was first dissolved at a concentration of 20 mg/mL (batch no. 111 and 112) or 33 mg/mL (batch no. 342) in deuterated water with HCl to ensure stoichiometric solubilization of the polymer. The mixture was freeze-dried three times, to exchange labil protons by deuterium atoms. Proton magnetic nuclear resonance measurements were performed at 303 K, using deuterated water as solvent. Degrees of acetylation were found to be 13.8%, 2.9%, and 20%, respectively.

Molecular weights were assessed by size exclusion chromatography and multiangle laser light scattering (MALLS) using TSK-gel G-4000 PWXL and G-6000 PWXL columns and an IsoChrom LC pump (Spectra Physics). The columns were connected to a Waters 410 (Waters-Millipore) differential refractometer. CH_3COOH-ammonium acetate buffer at pH 4.3 was used as an eluent. MALLS detection was obtained by means of a Wyatt Dawn F detector on-line, operating at 632.8 nm. The polymer solutions (0.1% w/v) were filtered on a 0.22 μm pore size cellulose acetate membrane (Millipore) before injection using an injection loop (50 μm). Molecular weights (in weight) of chitosan were found to be 520,000 g/moL, 451,000 g/moL, and 180,000 g/moL, for batch no 111, 112, and 342, respectively

Methods

Preparation of Solutions. Chitosan powder, distilled water and bromothymol blue 0.04% wt (Sigma-Aldrich) were mixed. Due to the transition interval of the color indicator, related to the pH range 6–7.6, the mixture was blue. Then, acetic acid (Laurylab) was added to achieve protonation and thus,

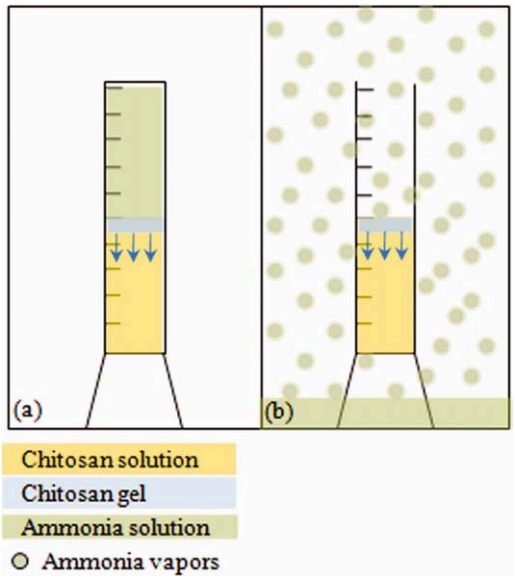

Figure 1. Schematic of the wet and the vapor gelation processes.

(a) wet gelation process. (b) vapor gelation process. [Color figure can be viewed in the online issue, which is available at wileyonlinelibrary.com.]

solubilization of the polymer, which lead to the final yellow solution. The chemical reaction occurring is as follows:[14]

$$\text{Chit} - \text{NH}_2 + \text{AcOH} \Leftrightarrow \text{Chit} - \text{NH}_3^+ + \text{AcO}^- \qquad (1)$$

where Chit-NH_2 is the chitosan under insoluble form, and AcOH is the acetic acid. Chit-NH_3^+ is the quaternium chitosan, soluble in water, and AcO^- is the acetate ion.

Final chitosan concentrations were equal to 2% w/v and 3% w/v, based on preliminary tests. Below 2% or 3% w/v depending on the batch, the mechanical properties of the final gels were not sufficient. For larger polymer concentrations, the final solutions were too viscous and it was hard to obtain a homogeneous casting. Solutions were then stirred for 24 h and stored at 277.15 K until use.

Gelation of Chitosan Solution Using the Wet Gelation Process. Ammonia was used as the chemical gelation agent. It was used in diluted ammonia aqueous solutions (Laurylab) at different initial concentrations varying from 0.32 mol/L to 2.59 mol/L. These gelation conditions correspond to concentration ranges previously used[7] or reported in literature.[12]

Chitosan solution (5 cm^3) were first poured into a graduated measuring tube; then 5 cm^3 of ammonia solution were carefully added to the polymeric solution, using a needle, not to disturb the liquid/liquid interface and to ensure a regular diffusion through it (Figure 1a).

The displacement of the gelation front was followed with a camera, taking pictures at regular time steps, throughout the gelation process. These photos were then analyzed using ImageJ® software to plot gelation kinetics. The different operating conditions are gathered in Table 1.

Gelation of Chitosan Solution Using the Vapor Gelation Process. In the case of the vapor process, ammonia vapors were used as the gelation agent under different partial pressures. 5 cm^3 of chitosan solution were poured into a graduated measuring tube immersed in a thermostated water bath, at the same temperature as the one of the gelation chamber atmosphere. In that configuration, heat transfers occurring during gelation were mainly due to ammonia intake and water outflow at the upper interface of the polymeric system. Hence, heat conduction through lateral surface of the graduated measuring tube was neglected.

The tube was then exposed to ammonia vapors (Figure 1b) generated in a thermostated double walled closed chamber (Legallais, France), containing an ammonia aqueous solution (Figure 2). The whole system (polymeric solution in the tube) was placed onto an inox plate. Using a balance (Precisa XB 320 M, Balco) and a data acquisition system (Balint software), the mass variations occurring during gelation could be monitored in-line and gravimetric measurements were performed for investigating global mass transfer phenomena.[14] The whole operating conditions are gathered in Table 2.

Table 1. Operating Conditions

	Experiment	Batch	Chitosan Concentration (% w/v)	DA (%)	Temperature (K)	Ammonia Concentration (mol L^{-1})	Ammonia Partial Pressure (Pa)
Wet gelation process	A	342	3	20	287	0.32	/
	B	342	3	20	287	0.64	/
	C	342	3	20	287	1.29	/
	D	342	3	20	287	1.94	/
	E	342	3	20	287	2.59	/
	T1	342	3	20	287	1.29	/
	T2	342	3	20	301	1.29	/
	T3	342	3	20	309	1.29	/
	DA1	111	2	13.8	301	1.29	/
	DA2	112	2	2.9	301	1.29	/
	DA3	342	2	20	301	1.29	/
Vapor gelation process	F	342	3	20	293	/	1346
	G	342	3	20	293	/	2020
	H	342	3	20	293	/	2946
	I	342	3	20	293	/	3367
	J	342	3	20	293	/	4200
	T4	342	3	20	293	/	2946
	T5	342	3	20	301	/	4342
	T6	342	3	20	309	/	6249
	DA4	111	2	13.8	301	/	4342
	DA5	112	2	2.9	301	/	4342
	DA6	342	2	20	301	/	4342

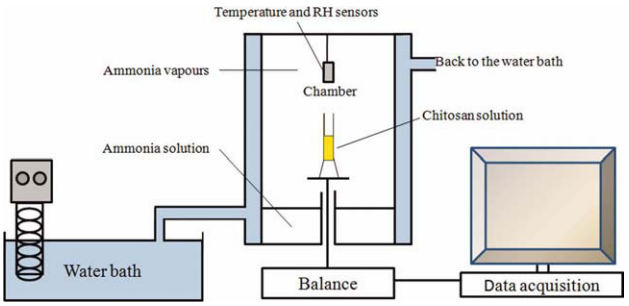

Figure 2. Schematic of the vapor process.

[Color figure can be viewed in the online issue, which is available at wileyonlinelibrary.com.]

Calorimetric Measurements. Calorimetric measurements were performed to improve the modeling of heat transfers occurring during the gelation. The experimental process involved (i) a tailor-made calorimeter, (ii) a resistance-heated (Bioblock Scientific, Polystat μpros) bath of distilled water coated with a polystyrene packaging, (iii) a temperature sensor with a 0.01 K precision (Almemo 2290-8) measuring temperature within the calorimeter and (iv) a data acquisition system (Data Control) recording temperature changes. Tests were divided into several steps to evaluate the heat capacity of the calorimeter, the enthalpy of reaction between acetic acid and ammonia, the heat capacity of a chitosan solution and the gelation heat. Details of each measurement and numerical data are provided in Appendix A.

Theory

The mathematical model dedicated to the chitosan gelation process, involving a coupling between mass and heat transfers and chemical reactions, has been described in a previous paper;[14] hence the architecture of the model has not been detailed in this article, but the main equations have been summarized in a table. Nevertheless, the previous model was limited to the vapor gelation process conducted for conditions of free convection in the external bulk environment. This article aims at investigating the wet process as well, conducted in various conditions of hydrodynamics in the bulk liquid phase in contact with the chitosan solution. Therefore, the description of the boundary conditions applied during the wet process must be expressed properly, whatever the hydrodynamic conditions imposed in the surrounding liquid phase (free or forced convection).

Geometry of the models

The geometries associated to both gelation processes are illustrated in Figure 3. In wet process, the polymeric system is initially poured in a graduated measuring tube. Then, an aqueous solution of ammonia is added very smoothly above the biopolymer solution to prevent a mixing between the two liquid phases. Once the ammonia comes into contact with the chitosan solution, concentration gradients appear between both phases for each component, leading to mass transfers by molecular diffusion through the liquid/liquid interface. Both phases are characterized by the ammonia and water activities, a_a and a_w, respectively.

In the vapor gelation process, the gelation rate is controlled by an ammonia inflow through the gas/solution interface. Gas phases over and below the system are characterized by the following parameters: the bulk temperature T_b (K), the relative humidity, RH (%), the vapor pressure of each volatile compound P_{vi} (Pa) and the heat transfer coefficients h_b^{up} and h_b^{down} (W/m^2 K).

The assumptions corresponding to wet and vapor gelation models are: (1) one-dimensional Fickian diffusion; (2) no influence of chitosan on the activity of the other species; (3) no influence of chitosan polymer chains on the transport mechanisms of small species.

For the wet process, a uniform temperature was assumed in the system whereas for the vapor process, the enthalpy contributions of the mass transfers at the air/solution interface were taken into account. Three other assumptions have to be considered for the vapor process; they are detailed in the previous study.[14]

Thermodynamic model

To simulate the wet process, a continuity condition was assumed at the liquid/liquid interface.

Table 2. Mass Transfer Models Related to the Different Compounds Involved

		Wet Gelation Process				Vapor Gelation Process		
		Initial Condition $\rho_i^\eta(0) =$	Boundary Conditions Neumann Conditions: $J_i(\eta) =$			Initial Condition $\rho_i^\eta(0) =$	Boundary Conditions Neumann Conditions: $J_i(\eta) =$	
Compound	Local mass balance	$t = 0$	$\eta = 0$	$\eta = 0.5$	$\eta = 1$	$t = 0$	$\eta = 0$	$\eta = 1$
NH_3	$\frac{\partial \rho_1}{\partial t} - \frac{D_{1/m}}{H_s^2}\frac{\partial^2 \rho_1}{\partial \eta^2} = R_1$	0	0	J_{1/amm_sol}	0	0	0	$k_1\left[\rho_1^e(T_b) - \rho_1^i(T)\right]$
H_2O	$\frac{\partial \rho_2}{\partial t} - \frac{D_{2/m}}{H_s^2}\frac{\partial^2 \rho_2}{\partial \eta^2} = 0$	ρ_{20}^η	0	J_{2/amm_sol}	0	ρ_{20}^η	0	$k_2\left[\rho_2^e(T_b) - \rho_2^i(T)\right]$
$ChitNH_3^+$	$\frac{\partial \rho_3}{\partial t} = R_3$	ρ_{30}^η	0	0	0	ρ_{30}^η	0	0
$ChitNH_2$	$\frac{\partial \rho_4}{\partial t} = R_4$	ρ_{40}^η	0	0	0	ρ_{40}^η	0	0
AcOH	$\frac{\partial \rho_5}{\partial t} - \frac{D_{5/m}}{H_s^2}\frac{\partial^2 \rho_5}{\partial \eta^2} = R_5$	ρ_{50}^η	0	J_{5/amm_sol}	0	ρ_{50}^η	0	0
AcO^-	$\frac{\partial \rho_6}{\partial t} - \frac{D_{6/m}}{H_s^2}\frac{\partial^2 \rho_6}{\partial \eta^2} = R_6$	ρ_{60}^η	0	J_{6/amm_sol}	0	ρ_{60}^η	0	0
NH_4^+	$\frac{\partial \rho_7}{\partial t} - \frac{D_{7/m}}{H_s^2}\frac{\partial^2 \rho_7}{\partial \eta^2} = R_7$	0	0	J_{7/amm_sol}	0	0	0	0

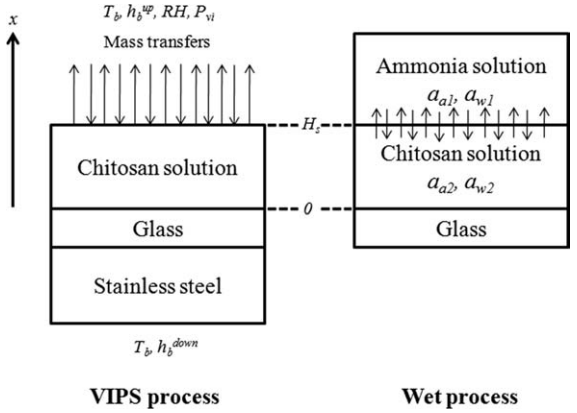

Figure 3. Geometries of the models.

Concerning the vapor gelation process, the gas-liquid equilibrium data of the ammonia-water system were used.[25] Indeed, the chitosan concentration was very low (2–3% w/v) and the interaction parameters between—chitosan and water—and—chitosan and ammonia—have not been reported in the literature.

Mass transfer model coupled to chemical reactions

The local continuity equation for each component was written as follows, assuming a binary Fickian diffusion within the polymer matrix

$$\frac{\partial \rho_i}{\partial t} + \frac{\partial}{\partial x}\left(-D_{i/m}\frac{\partial \rho_i}{\partial x}\right) = R_i \quad 1 \text{ to } 7 \tag{2}$$

Besides, in this article, a coordinate transform was performed to facilitate the numerical resolution and the comparison between both geometries (film vs. cylindrical)

$$\eta = \frac{x}{H_s} \tag{3}$$

H_S is the position of the upper interface in contact with the phase containing ammonia (gas or liquid phase depending on the gelation process). The position of the upper boundary was fixed and a constant mutual diffusion coefficient in the polymer solution, $D_{i/m}$ (m^2/s), was assumed.

The reaction term R_i took into account both reactions of ammonia (NH_3) with acetic acid (AcOH) and protonated chitosan (Chit-NH_3^+), leading to the formation of acetate ion (AcO^-), insoluble chitosan (Chit-NH_2) and ammonium ion (NH_4^+).

The PDE describing the mass transfer phenomena were reminded in Table 2. The initial and boundary conditions are rapidly discussed in the following sections (especially for the wet process, which was not simulated in the previous paper).

- Initial conditions:

For both gelation processes, there was no ammonia nor ammonium ion within the polymeric system at initial time. Nevertheless, due to Eq. 1, the polymeric system initially contained small amounts of both chitosan under insoluble form and acetic acid.

- Boundary conditions:

Considering the wet gelation process, continuity conditions were assumed at the interface between the chitosan solution and the ammonia bath (at the position $\eta = 0.5$), while impermeable interfaces were considered at the bottom of the domain ($\eta = 0$, polymer solution/substrate interface) and at the upper interface ($\eta = 1$, ammonia solution/ammonia bath interface).

In vapor gelation process, impermeable interface was considered at the bottom of the domain ($\eta = 0$, polymer solution/substrate interface) while flux conditions (Neumann boundary conditions) were assumed at the upper surface ($\eta = 1$, polymeric solution/air interface).

Heat transfer model

A heat transfer model was coupled to the mass transfer model dedicated to the vapor process for three main reasons:

1. In vapor gelation process, mass transfers including phase change occurred at the upper interface. Endothermic absorption and exothermic evaporation should be taken into account,
2. The external mass transfer rates depend on the air motion above the air/solution interface and on the molecular diffusion of transferring components through the boundary layer. In conditions of free convection, the driving force for air motion is the air density gradient between the interface and the bulk, which is mainly controlled by the temperature gradient. Consequently, the heat transfer rate should be calculated to properly describe the external mass transfer rate.
3. The chemical reactions involved in the gelation process could be endo- or exothermic.

In the case of thin films, uniform temperature in the whole sample was assumed in most of cases, since the heat transfer by conduction within the sample was generally much faster than the heat production due to mass exchanges. A lumped parameter approach is thus sufficient to simulate the temperature variation of the system.[26,27] For cylinder geometry (deeper samples), the thickness is too high to ensure uniform temperature in the whole sample, therefore the heat equation should be solved

$$\rho_i Cp_i \frac{\partial T}{\partial t} - \nabla \lambda_i \nabla T = Q \tag{4}$$

where ρ_i (kg/m^3), Cp_i (J/kg K), and λ_i (W/m K) were the density, the heat capacity and the thermal conductivity of i, respectively. Q (W/m^3) was a heat source term (production or consumption).

Diffusion formalism

Diffusion through the gel was assimilated to diffusion through water, since the polymer concentration was very low in the initial polymeric solution and in the forming gel ($[water]_{gel\ or\ solution} > 96\%$ w/v). Hence, in a first approach, diffusion coefficients in gel and aqueous phases were the same.[28] Diffusion coefficient of ammonia in water $D_{1/2}$ was calculated for each operating conditions, using Wilke and Chang correlation[29]

$$D_{1/2} = 7.4 \times 10^{12} \times \frac{(\varphi \times M_2)^{0.5} \times T}{\mu_2 \times V_1^{0.6}} \tag{5}$$

where ϕ was the association factor of water ($\phi = 2.6$), M_2 the molar mass of water (g/mol), μ_2 the viscosity of water (mPa.s) and V_1 (cm^3/mol) the molar volume of ammonia.

Mass and heat transfer coefficients

Mass and heat transfer coefficients for free convection have already been discussed in a previous paper,[14] but

specific correlations should be used to describe the external transfer phenomena in conditions of forced convection. Such semiempirical correlations are presented below:

• For the wet gelation process, a mechanical mixing in the ammonia bath was considered to enhance the mass transfer coefficients at the liquid/liquid interface. Therefore, a flux condition was applied at the liquid/liquid boundary ($\eta = 0.5$) and the flux J_1 (kg/m^2 s) was written as follows

$$J_1 = k'_1 \times \Delta\rho_1 \tag{6}$$

where k'_1 (m/s) was the mass transfer coefficient of ammonia in forced convection and $\Delta\rho_1$ (kg/m^3) was the gradient of ammonia concentration between both liquid phases. k'_1 could be expressed from the expression of the Sherwood number given by Asai et al. (1983)[30]

$$Sh = 0.0119 Sc_{sol}^{1/3} \mathrm{Ca}^{6/13} [\varphi^4 \times Re_{sol}^3 + Re_{NS}'^{8/3}]^{1/4} \tag{7}$$

$$k'_1 = \frac{Sh \times D_{1/2}}{L_c} \tag{8}$$

The semiempirical correlation involving the Sherwood number has been obtained in a liquid/liquid reactor without any break-up of the flat interface. In Eq. 7, Sc_{sol} and Re_{sol} represented the Schmidt number and the Reynolds number related to the chitosan solution. Ca was the capillary number between the chitosan solution and the nonsolvent ammonia solution, φ was a correction factor and Re'_{NS}, a modified Reynolds number in the ammonia solution

$$Re'_{NS} = Re_{NS} \times \frac{\nu_{NS}}{\nu_{sol}} \tag{9}$$

ν_{NS} and ν_{sol} (m^2/s) were the kinematic viscosities of the ammonia solution and of the chitosan solution, respectively. In this work, as there was no stirring of the chitosan solution, Eq. 7 could be re-written as follows

$$Sh = 0.0119 Sc_{sol}^{1/3} \mathrm{Ca}^{6/13} [Re_{NS}'^{8/3}]^{1/4} \tag{10}$$

• The conditions of forced convection could also be simulated for the vapor gelation process. The conditions of forced convection corresponded to an air flow rate conducted in laminar or turbulent hydrodynamic regime. The mass transfer coefficients could be calculated using the following correlation[23]

$$\frac{k_i L_c y_{air,lm}}{M_i D_{i/g}} = 0.27 \times Re^{0.5} Sc_i^{0.33} \tag{10}$$

The Reynolds number characterized the local hydrodynamics above the interface and was expressed by

$$Re = \frac{\rho_g \times u_\infty \times L_c}{\mu_g} \tag{11}$$

where ρ_g (kg/m^3) was the density of air, L_c (m) was the characteristic length of the system (casting film diameter) and μ_g (Pa s) was the viscosity of the gaseous phase.

Parameter determination

The parameters such as the molar mass, molar volume and the density of each constituent as well as the viscosity of solvent were taken from handbook.[25,31] The thermal parameters such as the heat capacity and the enthalpy of reactions (ΔH_R) were estimated by dedicated experiments (cf. Appendix A). With regards to the water volume fraction in the chitosan solution or gel, the other thermal parameters were assumed to be the same as for pure water. Other physical parameters (thermal conductivity of glass or stainless steel, vaporization enthalpy of water and ammonia) were found in literature.[31] Concerning the diffusion formalism, the association factor for water was found in literature too.[32]

The values of the reaction rate constants were estimated from the paper of Eigen and De Maeyer (1955).[33] These authors aimed at investigating the rate of the neutralization reaction between H_3O^+ and OH^- from time dependence of the dissociation field effect; they determined a rate constant $k = 1.3\ 10^{11}$ L/mol s. The same order of magnitude was also considered in our study for the reverse and forward constant rates of reactions of NH_3 with the acidic species present in chitosan solutions (acetic acid, protonated form of chitosan). Indeed, protons exchanges are also involved in these reactions. Based on the work of Eigen and De Maeyer (1955), a global reaction order of two was considered, one for each reactant. Although the literature is poor concerning the reaction rate constants in the case of acid/base reactions, one specific study carried out almost three decades ago highlighted that protonation of macromolecules was very fast.[34] The authors analyzed the kinetic of the protonation of a surface group of a neutral red. They mentioned that the proton emitter could be excited, dissociated and decayed to the ground-state anion within 30 ns. Such a study was in agreement with the aforementioned work of Eigen and De Maeyer and confirmed that the reaction rates involved in our system are expected to be very fast.

The physical parameters (density, viscosity and thermal properties of gas and liquid phases) used in the external mass transfer equations were estimated by expressions depending on the temperature from handbook.[25] The characteristic length of the interface (L_c) was measured. It represented the equivalent diameter of the transfer area. The value of the relative humidity in the gelation chamber was experimentally determined for each gelation experiment. The bulk temperature was maintained constant thanks to a double wall chamber. Therefore, no adjustable parameters were used in the model to fit the experimental data. The numerical values of the parameters used in the model are gathered in Table 3.

Numerical algorithm

The system of partial differential equations describing the coupling between the chemical reactions and mass and heat transfer phenomena were numerically solved in one-dimension (x-axis) using finite element software: COMSOL Multiphysics® 3.5a. The mesh was refined where the concentration gradients were expected to be the highest, i.e. the interface regions ($\eta = 0.5$ for the wet gelation process and $\eta = 1$ for the vapor gelation process). In addition, a variable time step was used to improve the numerical resolution.

Results and Discussion

Both gelation processes are induced by the penetration of ammonia within the chitosan solution. Since ammonia

Table 3. Values of Physical Parameters Used in Gelation Simulation

Parameter	Value	Units	Reference
Cp_{chit}	4650	J/kg.K	Measured
Cp_g	750	J/kg.K	31
Cp_{ss}	510	J/kg.K	31
Cp_w	4184	J/kg.K	31
$D_{2/g}$	2.58×10^{-5}	m^2/s	25
g	9.81	m/s^2	25
pK_{a1}	9.3	/	35
pK_{a2}	6.5	/	35
pK_{a3}	4.75	/	35
ΔH_R	932.8×10^3	J/kg	Measured
ΔH_{v1}	1371.2×10^3	J/kg	25
ΔH_{v2}	2256×10^3	J/kg	25
k_j^f	# 10^{11}	L/mol s	33,34
k_j^r	# 10^{11}	L/mol s	33,34
L_c	13×10^{-3}	M	Measured
M_1	17×10^{-3}	kg/mol	25
M_2	18×10^{-3}	kg/mol	25
M_3	162×10^{-3}	kg/mol	35
M_4	161×10^{-3}	kg/mol	35
M_5	60×10^{-3}	kg/mol	25
M_6	59×10^{-3}	kg/mol	25
M_7	18×10^{-3}	kg/mol	25
V_1	24.93	cm^3/mol	31
RH	>96	%	Measured
Φ	2.6	/	32
λ_a	0.026	W/m K	31
λ_g	1.05	W/m K	31
λ_{ss}	16	W/m K	31
λ_2	0.6	W/m K	31
ρ_a	1.293	kg/m^3	31
ρ_g	2230	kg/m^3	31
ρ_{ss}	7700	kg/m^3	31

#, order of magnitude.

diffused from the top to the bottom of the chitosan solution, a front of pH change appeared and moved through the solution. In the polymeric system, the local value of the pH could be calculated using the following expressions, which represented (1) the ammonia dissociation, (2) the deprotonation reaction of chitosan and (3) the neutralization of acetic acid in excess.

$$\begin{aligned} \mathrm{pH} &= \mathrm{p}K_{a1} + \log\frac{\mathrm{NH_3}}{\mathrm{NH_4^+}} = \mathrm{p}K_{a2} + \log\frac{\mathrm{Chit-NH_2}}{\mathrm{Chit-NH_3^+}} \\ &= \mathrm{p}K_{a3} + \log\frac{\mathrm{AcO^-}}{\mathrm{AcOH}} \end{aligned} \quad (12)$$

where pK_{a1}, pK_{a2}, pK_{a3} were the negative logarithms of the dissociation constants of NH_4^+/NH_3, Chit-NH_3^+/Chit-NH_2 and $AcOH/AcO^-$.

At the top of the domain, the pH became higher than neutrality whereas at the bottom it was still lower than neutrality because ammonia had not reached this region yet. As soon as the pH increased and overcame neutrality, the deprotonation reaction between ammonia and Chit-NH_3^+ occurred. The displacement of the pH front was experimentally followed using a color indicator added during the preparation of the initial polymer solution. The color indicator had to be chosen so that the equilibrium constant (pK_a) of the chitosan was included in its transition range. Since the pH change was locally very abrupt (from an acid to a basic pH), the color change was associated to the gelation, meaning that the gelation front could be followed by an optical method using an in-line and non destructive method. This is a classic procedure reported in polymer engineering.[36–38] For instance, the precipitation front move was previously monitored in the formation of polyethersulfone films[36] and polyphthalazine ether sulfone ketone membranes.[37,38] In those studies, the precipitation front was due to diffusion of nonsolvent into the synthetic polymeric system. In our work, chemical reactions were also involved. Moreover, to improve the monitoring of these gelation fronts, the color indicator permitted to clearly distinguish the interface between the chitosan gel and the chitosan solution.

On the gelation using the wet gelation process

Gelation using the wet process was based on liquid/liquid exchanges and involved three main phenomena: (i) the transfer of ammonia between two liquid phases, (ii) its diffusion through the polymeric system and (iii) a chemical reaction between ammonia and Chit-NH_3^+.

The moving of the gelation front was experimentally observed in an expanded geometry (cylinder) and presented in Figure 4. At each time step, the relative position of the gelation front was calculated, until the front reached the bottom of the polymeric system. The corresponding points were plotted in Figure 5 for increasing ammonia concentrations in the ammonia bath. Greater the initial ammonia concentration in the ammonia bath, greater the initial driving force for NH_3 mass transfer, keeping all the other parameters constant. Thus, Figure 5a showed that gelation front moved faster when increasing the initial ammonia concentration. To investigate the nature of the limiting phenomenon to the whole gelation process, we reported the half-gelation time (time needed to turn half the initial solution depth into a gelled system) vs. the initial ammonia concentration. Figure 6a also showed that the half gelation time tended toward an asymptotic value (value $t_{\eta=0.25} = 15$ h) when the ammonia concentration exceeded 1.29 M. Then, the gelation time could not be drastically reduced even by increasing the initial driving force to mass transfers. This point is important for further industrial issues since the gelation time should be optimized to optimize the operating costs.

On the gelation using the vapor gelation process

The vapor gelation process involved the exposure of the chitosan solution to ammonia vapors. Compared to the wet process, the vapor gelation process was weakly different since it involved: (i) ammonia transport in gas phase to the gas/liquid interface, (ii) gas/liquid transfer at the interface, (iii) ammonia diffusion through the polymeric system coupled to (iv) chemical reaction between ammonia and Chit-NH_3^+. Thus, another phenomenon could contribute to the whole mass transfer resistance: the solubility of ammonia in the chitosan solution.

As exposed in the previous section, gelation time was experimentally followed by the vapor gelation process too. Figure 5b presents gelation kinetics obtained from five increasing partial pressures of ammonia in gas phase above the system. It exhibited that an increase of P_{NH3} led to a faster gelation in the range [1300–4200 Pa]. Besides, as highlighted in Figure 6b, the decrease of the half-gelation time was faster for the lowest ammonia partial pressures

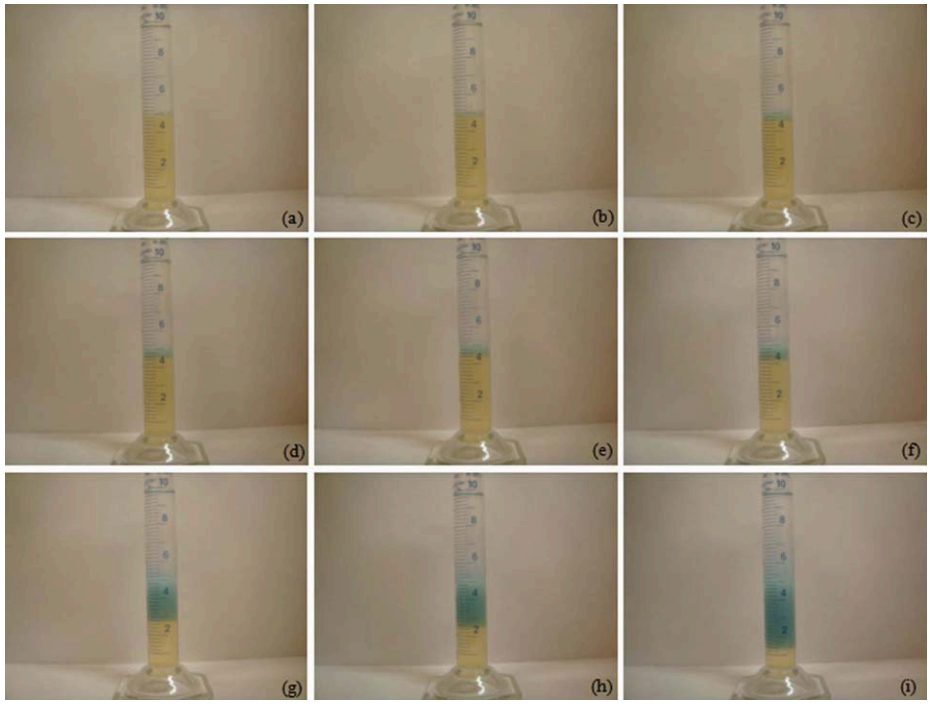

Figure 4. Gelation fronts observed in the wet gelation process.

[NH_3] = 1.29 M. (a) $t = 0$. (b) $t = 5$ min. (c) $t = 30$ min. (d) $t = 45$ min. (e) $t = 1$ h. (f) $t = 2$ h. (g) $t = 15.5$ h. (h) $t = 19.5$ h. (i) $t = 42$ h. [Color figure can be viewed in the online issue, which is available at wileyonlinelibrary.com.]

($P_{NH3} < 2020$ Pa). Indeed, from $P_{NH3} = 2000$–3300 Pa, the half-gelation time was reduced by only 20% and from $P_{NH3} = 3300$–4200 Pa, its value remained constant. This result pointed out that the molecular diffusion of ammonia within the chitosan matrix controlled the whole gelation kinetics, therefore the transport by molecular diffusion within the chitosan matrix could be considered as the main resistance to gelation.

Comparison of gelation kinetics involved in the wet and the vapor gelation processes

The main difference reported in literature for synthetic polymers between wet and the vapor processes concerned the characteristic times involved in phase separation mechansisms.[10] The wet process is very fast and often leads to macrovoïd structures,[39,40] whereas the vapor process (VIPS) induces a strong reduction of the mass transfer rates, and leads to the formation of more uniform porous structures.[24] More precisely, the vapor process applied to other polymeric systems including for instance, poly(ether-imide),[9] polysulfone[41] (phase separation process) or chitin[15,16] (gelation process) was reported to be the best way for controlling the mass transfer rates and thus the structuring mechanisms too.

In the case of chitosan gelation, a comparison of wet and vapor processes was only possible considering similar driving forces for mass transfers. This condition was reached by calculating the ammonia concentration in liquid phase in equilibrium with a given ammonia partial pressure. At thermodynamic equilibrium, characterized by Henry's law, it was possible to calculate the corresponding ammonia concentration in liquid phase. Consequently, the gelation time obtained for wet and the vapor gelation processes could be plotted using the same x-axis (Figure 6). For similar sample thicknesses and similar chemical potential of ammonia in the ammonia medium (liquid bath for the wet process and gas phase for the vapor gelation process), similar gelation times were obtained in the range [2000-3500 min]. These curves pointed out that the two gelation processes were almost the same considering mass transfer rates. This result was totally different from the results reported in literature on the elaboration of polymeric matrices by nonsolvent penetration. This difference can be explained by the initial system configuration: on the one hand, the solvent was an acid aqueous solution that mainly contained water (its initial concentration in the chitosan solution was high than 96% w/v); On the other hand, the chemical potential of ammonia was high in the ammonia medium whatever the gelation process (ammonia bath or gas phase). Indeed, in wet process, NH_3 was diluted in an aqueous solution (ammonia bath), i.e. its concentration was low and the water chemical potential was very high. In vapor gelation process, the gas phase, which contained ammonia vapors, was almost saturated by water, characterized by a relative humidity higher than 95%. Thus, for both processes, the driving force for the solvent extraction and the water evaporation was very low and led to very slow transfer of solvent (water) between the ammonia medium and the chitosan solution. For that reason, identical driving force for ammonia transfer (identical chemical potential of NH_3) led to similar transfer rates of NH_3 through the chitosan solution. Moreover, since the chemical reaction involved in the gelation were fast, the curves representing the half-gelation times vs. the ammonia concentration exhibited similar trends whatever the process.

Influence of temperature on gelation kinetics

It was expected that the temperature could influence the gelation mechanisms since (i) it could affect the external

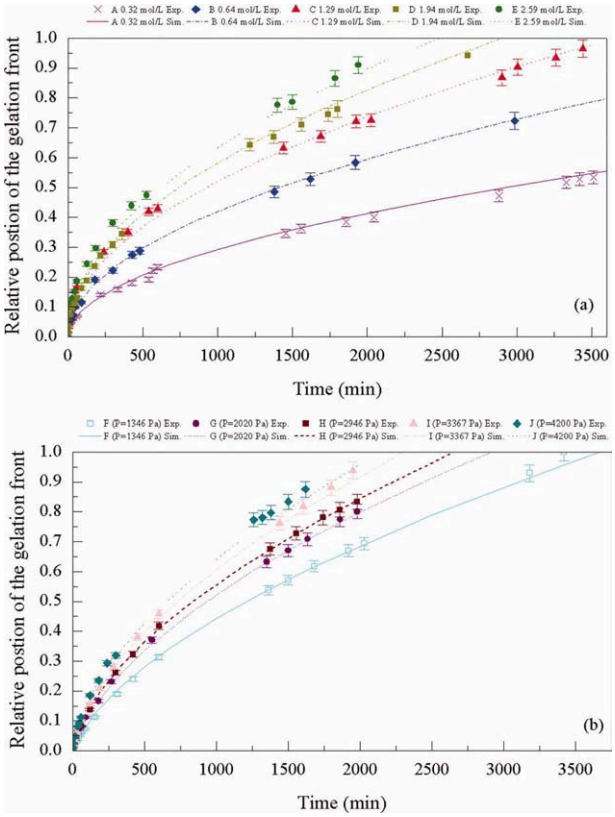

Figure 5. Experimental and simulated gelation kinetics.

(a) wet gelation process: Batch 342, [chitosan] = 3.00% w/v. (b) vapor gelation process: Batch 342, [chitosan] = 3.00% w/v. [Color figure can be viewed in the online issue, which is available at wileyonlinelibrary.com.]

mass transfer coefficient, especially for conditions of natural convection, (ii) the diffusion coefficients of small species clearly depend on the temperature and (iii) the temperature could affect the polymer chain mobility.

In wet gelation process, a temperature increase led to an increase of the diffusion coefficients and consequently the gelation rate. In vapor gelation process, a temperature change was expected to affect not only the diffusion coefficients, but also the initial driving force to mass transfer. Therefore, the role of the temperature on the gelation rate was investigated for a high P_{NH3} value because we previously showed that for the highest ammonia partial pressure in the gaseous phase ($P_{NH3} > 2020$ Pa), the gelation time kept an asymptotic constant value. By this way, the temperature was expected to affect only the diffusion rate and the chain interactions, but not the external transfer rate.

In the temperature range tested in this study [287–309 K], Figures 7a and 7b show that an increase of T automatically induced a decrease of gelation rate from about 3500 min (58.3 h) to 2300 min (38.3 h) for the wet gelation process, and from 2600 min (43.3 h) to 1600 min (26.7 h) for the vapor gelation process. Such results were in good agreement with previous works. Indeed, Liu and Gao (2003) have highlighted an increase of the mutual diffusion coefficients with increasing temperature in various polymeric solutions.[42] Reis et al. (2005) have investigated the influence of the temperature of self and mutual diffusion coefficients in polymeric solutions,[43] and they argued that the essential features of diffusion in the polymeric solution involved segmental mobility and constrains due to chain connectivity and chain entanglements. This second statement was also reported by Tonge et al. (2000) who have studied the diffusion of camphorquinone in poly(methyl methacrylate)/methyl isobutyrate matrices as a function of temperature in the range [298 K – 323 K].[44] Later, Chenite et al. (2006) studied the gelation of chitosan solutions via enzymatic hydrolysis of urea and observed an exponential decrease of gelation time with temperature.[45] In the present work, the temperature played a key role on chitosan polymer itself, by increasing the mobility of the polymer chains, and therefore the contact probabilities between Chit-NH_3^+ and NH_3. At the same time, an increase of temperature enhanced the molecular diffusion rate of ammonia through the polymeric matrix.

Influence of the acetylation degree on the gelation time

Despite the crucial role of degree of acetylation (DA) on chitosan properties,[46,47] its influence on the gelation rate had never been reported in the literature. Increasing the degree of acetylation lead to increasing the number of free amino groups, and thus to modifying the hydrophobic interactions with water. The DA defines the initial amount of protonated functions Chit-NH_3^+ and should also be related to chemical reaction involved in the gelation process. Figures 7c and 7d reported the gelation rates in wet and vapor gelation processes, respectively, and for three polymeric solutions obtained from three different chitosan. Either using the wet or the vapor gelation process, the same trend was observed, highlighting a weak influence of the DA on gelation rate. Increasing the DA led to reducing the number of amine functions and thereby to increasing the protonated functions on the chitosan polymeric chains; as a consequence more ammonia molecules are needed to induce the gelation and the gelation time is slightly reduced. Low DA involves high charge density, which is responsible for electrostatic repulsions; thus it prevents the formation of physical junctions between polymeric chains, and lead to delaying the gelation process. On the contrary, a higher DA reduces the charge density of the polymer and promotes the gelation mechanism. The same trend have been put in evidence by Montembault et al. (2005), who have investigated the gelation of

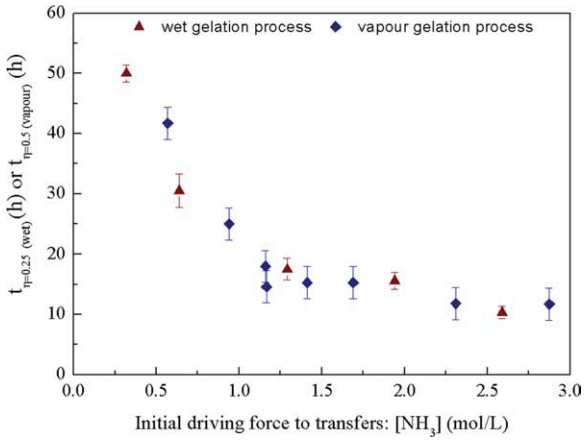

Figure 6. Gelation time of half the initial system height against initial ammonia concentration.

Batch 342, [chitosan] = 3.00% w/v. [Color figure can be viewed in the online issue, which is available at wileyonlinelibrary.com.]

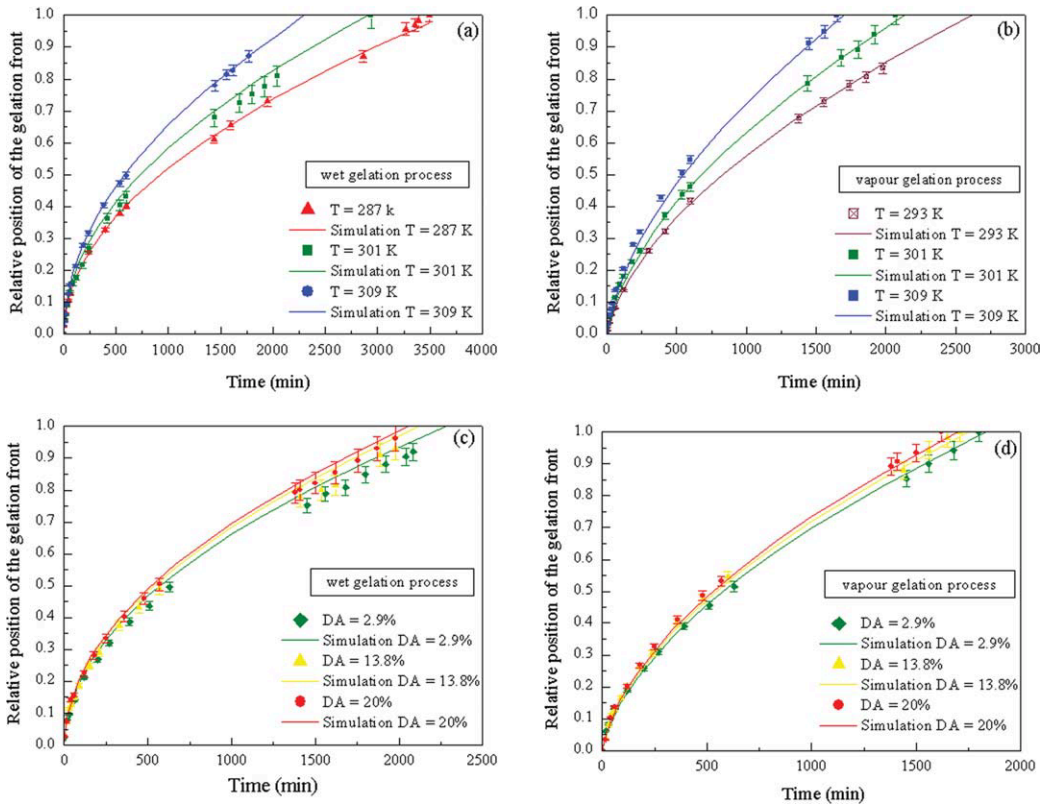

Figure 7. Influence of operating conditions on gelation kinetics.

(a) Influence of temperature in the wet gelation process: Batch 342, [chitosan] = 3.00% w/v. (b) Influence of temperature in the vapor gelation process: Batch 342, [chitosan] = 3.00% w/v. (c) Influence of degree of acetylation in the wet gelation process: [chitosan] = 2.00% w/v. (c) Influence of degree of acetylation in the vapor gelation process: [chitosan] = 2.00% w/v. [Color figure can be viewed in the online issue, which is available at wileyonlinelibrary.com.]

chitosan characterized by various DA in aqueous solution and using a rheometer.[12]

To conclude, before the preparation of chitosan matrices, it was shown that the DA has to be considered with special attention because its value affected not only the polymer biological properties but also the whole gelation rate.

Simulation results

Validation of the Model. Once the PDE of the numerical model were solved using COMSOL Multiphysics® 3.5a, the simulation results were validated for both processes using experimental data (cf. Figures 5 and 7). A good agreement was observed between both curves, whatever the operating conditions (T, P_{NH3}) and the initial formulation (polymer concentration, DA). Moreover, since the model involves external mass transfers (free convection), internal mass transport (molecular diffusion) and chemical reactions, such experimental validation using local data collected in-line (moving rate of the gelation front) were more reliable than an experimental validation using only global data (global mass loss or gain for instance). In addition, the model was validated for various operating conditions, proving its reliability. Lastly, all the parameters were determined experimentally or found in the literature, therefore no adjustable parameter was used for fitting the experimental curves. As a consequence, the numerical simulations were then used:

- to improve the understanding of the coupling between the elementary mechanisms involved in the gelation processes,
- to predict the gelation rate in various operating conditions.

Local Comparison of the Wet and the Vapor Gelation Processes. The experimental results exhibited that both gelation processes had similar characteristic times, depending on the operating conditions. The numerical model could also be helpful to predict the local concentration profiles through the sample thickness, at different time scales. Figure 8 reported the variation of pH and ammonia concentration profiles. In such cases, the optimal conditions of the driving forces to mass transfer were chosen for the simulations, i.e. when the gelation time stopped decreasing and reached a plateau. For constant temperature conditions and increasing time steps, Figure 8 highlighted similar ammonia penetration rates and similar progression rate of the pH fronts whatever the gelation process. These simulated results pointed out that because of the ammonia intake, the pH suddenly increased from 5.4 to 9 and then progressively increased above 10 in the region located next to the upper interface. Indeed, in the polymer solution, NH_3 formed NH_4^+ cation; since $pK_{a3} < pK_{a2}$, NH_3 also reacted with the acetate acid and then with the protonated form of chitosan (Chit-NH_3^+) to form Chit-NH_2. Once NH_3 had been consumed for the two acid-base reactions, it became in excess, and therefore the pH suddenly increased due to the predominance of the NH_3 form in solution leading to a progression of the pH front from the top to the bottom of the domain. It can be assumed that the pH front corresponds to the gelation front not only because the chemical reactions of deprotonation are very fast but also because

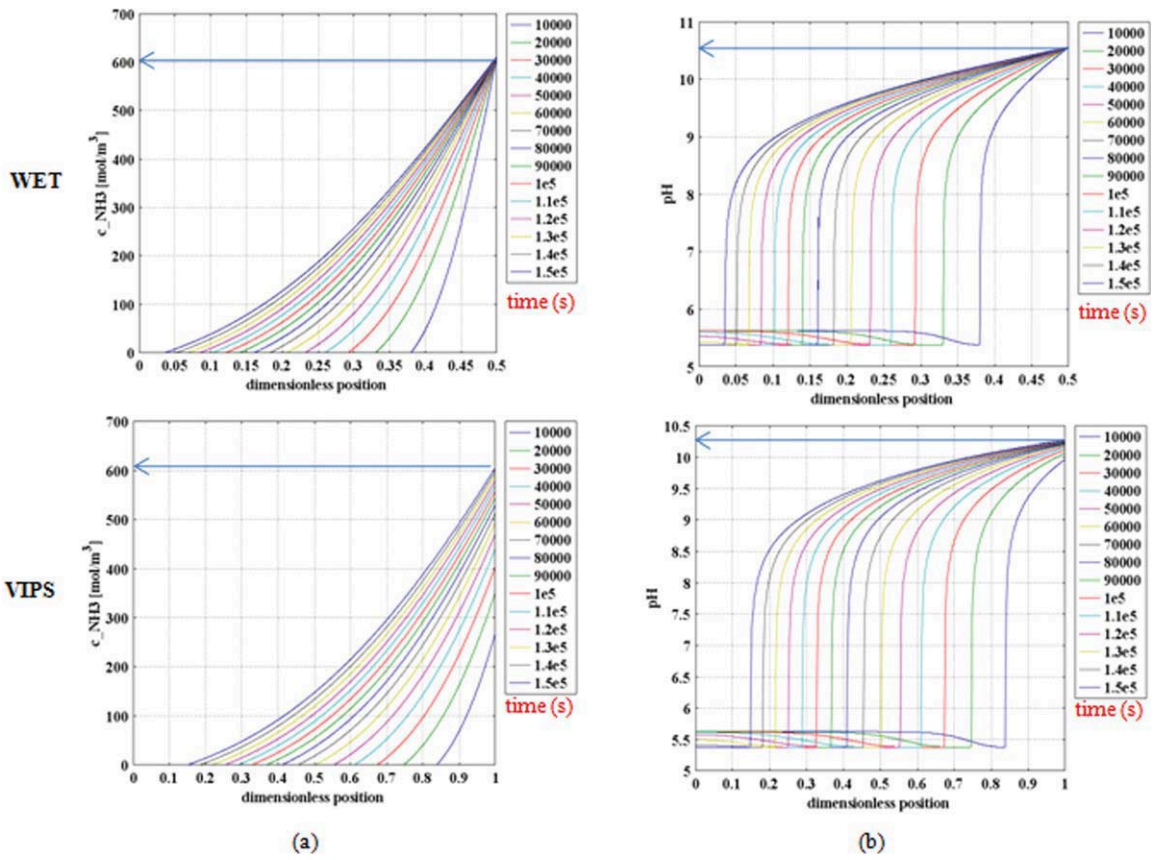

Figure 8. Local transfers involved in gelation of chitosan matrices by wet and vapor gelation processes.

Vapor gelation process: P_{NH3} = 2000 Pa; wet gelation process: [NH_3] = 1.29 M; depth: 0.03767 m. (a) Ammonia concentration profiles. (b) pH profiles. [Color figure can be viewed in the online issue, which is available at wileyonlinelibrary.com.]

the bonds between neighboring chitosan chains were expected to be formed very quickly once Chit-NH_3^+ reacted with NH_3.

Effect of Temperature and Hydrodynamic Conditions in the Bulk Phase (Free or Forced Convection). The influence of forced convection conditions on the gelation rate was investigated in both wet and vapor gelation processes. All simulation cases were summarized in Table 4. In each case, the gelled thickness was calculated after a gelation time of 100 s; moreover, the time necessary to induce a complete gelation of the sample (100% of the sample thickness) was calculated. The gain of time to reach a complete chitosan gelation was then calculated for each case, by comparison with the "reference" case.

In wet process, the influence of the mixing intensity on the mass transfer coefficient was tested: run 1 corresponded to the "reference" case; it was conducted without stirring at 298.15 K. From run 2 to 8, the influence of the stirring rate was investigated and from 9 to 11, the influence of the temperature was tested. Run 12 corresponded to an increase of temperature in stirring condition. At constant temperature (298.15 K), as for the vapor process, applying a stirring in the ammonia bath led to increase the gelled thickness after 100 s and to decrease the gelation time for a complete sample gelation. Indeed, the reduction of the gelation time was respectively equal to 14.7%, 21.1%, 22.9%, 26.6%, 27.2%, and 27.9% when the impeller velocity was successively fixed to 1, 3, 6, 30, 60, 300 and 600 tours per minute. It was clear from such values that it was no more necessary to increase the impeller velocity more than 30 min^{-1} since the gain in gelation time was no more interesting. Besides, in conditions of free convection in ammonia bath, the process temperature strongly affected the gelation time: an increase of 5 K led to a decrease of 23.7% of the gelation time and an increase of 25 K to a decrease of more than half the gelation time (51.2%). In such a case, the temperature did not only influence the internal diffusion mechanisms (diffusion coefficient in the chitosan solution) but also the external mass transfer rate. Indeed, a temperature modification affected both the diffusion coefficients of the transferring species and the liquid viscosity in the bath, leading to increasing the mass transfer rate in the ammonia bath. As expected, when applying the stirring condition at high temperature, the gain in terms of gelation time was the highest (more than 60% comparing to the "reference" case). Nevertheless, the final choice concerning the process conditions should take into account the integrity of the chitosan solution. On the one hand, the stirring rate above the solution should be moderated and on the other hand the temperature should not be too high to prevent the polymer degradation. For these reasons, the numerical model could be very useful to determine the best operating conditions whatever the geometry and to estimate the process duration that would permit a complete gelation of the chitosan solution.

Concerning the VIPS process, the "reference" case was conducted in free convection for a sample temperature equal to 298 K (run 13). From run 14 to 18, increasing air velocities were simulated; from run 19 to 21, the influence of the sample temperature was tested, keeping the free convection conditions; run 22 corresponded to forced convection

Table 4. Gelation of Matrices in Forced Convection for Both Gelation Process (Wet and Vapor)

Run	Type of Convection	T_b (K)	u_∞ (m/s)	N (min^{-1})*	t_{VIPS} (s)	Depth Gelled (%)	Time Gain (%) (100% Gelled)
1	Free	298.15	/	/	100	42.0	
					545	100	/
2	Forced	298.15	/	1	100	42.1	
					465	100	14.7
3	Forced	298.15	/	3	100	45.4	
					430	100	21.1
4	Forced	298.15	/	6	100	46.8	
					420	100	22.9
5	Forced	298.15	/	30	100	48.6	
					400	100	26.6
6	Forced	298.15	/	60	100	49.0	
					397	100	27.2
7	Free	298.15	/	300	100	49.4	
					394	100	27.7
8	Free	298.15	/	600	100	49.5	
					393	100	27.9
9	Free	303.15	/	/	100	48.0	
					416	100	23.7
10	Free	313.15	/	/	100	54.1	
					329	100	39.6
11	Free	323.15	/	/	100	60.1	
					266	100	51.2
12	Forced	323.15	/	30	100	70.9	
					192	100	64.8
13	Free	298.15	/		100	28.7	
					738	100	/
14	Forced	298.15	0.2		100	31.1	
					673	100	8.8
15	Forced	298.15	0.4		100	33.9	
					615	100	16.7
16	Forced	298.15	0.6		100	35.5	
					588	100	20.3
17	Forced	298.15	0.8		100	36.5	
					571	100	22.6
18	Forced	298.15	1		100	37.3	
					558	100	24.4
19	Free	303.15	/		100	29.9	
					704	100	4.6
20	Free	313.15	/		100	31.4	
					665	100	9.9
21	Free	323.15	/		100	32.4	
					632	100	14.4
22	Forced	323.15	1		100	37.8	
					524	100	29.0

Initial solution thickness: 0.0025 m; Run 1 to 12: $[NH_3]_{bath} = 1.29$ mol/L; Run 13 to 22: $P_{NH3} = 2000$ Pa.

conditions conducted at the highest temperature (323.15 K). For constant ammonia partial pressure, switching from free to forced convection permitted to enhance the gelation rate, since the mass transfer coefficient was enhanced. For the ''reference'' case, 28.7% of the sample thickness was gelled after 100 s, whereas with increasing the air velocity above the polymer solution, it increased to 31.1% ($u_\infty = 0.2$ m/s), 33.9% ($u_\infty = 0.4$ m/s), 35.5% ($u_\infty = 0.6$ m/s), 36.5% ($u_\infty = 0.8$ m/s), and 37.3% ($u_\infty = 1$ m/s). The increase rate is higher for the lowest air velocities and once u_∞ is sufficiently high, the gain in terms of gelled thickness is lower. Similar results were observed on the time needed to reach a complete gelation (decrease of the gelation time of 8.8%, 16.7%, 20.3%, 22.6% and 24.4%, respectively for air velocities of 0.2, 0.4, 0.6, 0.8, and 1m/s).

The influence of the bulk temperature on the gelation time was also investigated, keeping first free convection conditions (run 19–21) and then keeping the highest air velocity (run 22). It was observed that higher the temperature, lower the gelation time: successive increases of 5 K, 15 K, and 25 K led to the gelation time decreases of 4.4%, 9.9% and 14.4%, respectively. As expected, increasing both the temperature and the air velocity led to the lowest gelation time (reduction of 29% comparing to the ''reference'' case).

Forced convection allowed reducing the mass transfer limitation at the gas/system interface, but it did not induce a decrease of the mass transfer resistance in liquid phase. Hence, comparing runs 14 and 18, a gain of 23.6% on the gelation depth was obtained for a same exposure time to vapors (100 s) and identical initial ammonia partial pressure ($P_{NH3} = 2000$ Pa) when increasing u_8 from 0 to 0.6 m/s. When keeping on increasing the air velocity from 0.6 to 1 m/s, the additional gain in terms of gelled thickness was only about 6% whereas the air velocity almost doubled. Similar conclusions could be done concerning the whole gelation time. Since the temperature affects the internal diffusion mechanisms, a temperature increase led to increasing the transfer rate within the solution and since the main limiting factor to gelation is the internal mass transfer by molecular diffusion, monitoring the temperature could be useful for increasing the gelation rate by vapor process.

Influence of Heat Transfers on Gelation. Experimental data did exhibit the influence of temperature on gelation rates; in the model, the expressions of the diffusion coefficients and the external mass transfer correlations must consequently be temperature-dependant. Moreover, due to endo- and exothermic contributions of the mass exchanges at the interface, temperature gradients could appear in the sample. In this work, due to the low sample thickness, such gradients are most of times moderate and they do weakly affect the internal transport properties. Nevertheless, in vapor process, the sample temperature can be modified due to the heat production or consumption and a temperature gradient can be formed in the boundary layer between the solution interface and the bulk gas phase. Such temperature variation must be taken into account into the mass transfer model because it can affect the external mass transport rates, especially for free convection. Lastly, the heat production (or consumption) due to the chemical reaction should be added to the heat balance, but a preliminary experimental work allowed neglecting their contribution for this specific system (cf. Appendix A).

Conclusions

A coupling approach (modeling and experimental) was developed in this work for investigating the gelation of chitosan solution by a basic medium placed in a liquid bath (wet process) or a gas phase (vapor gelation process) in contact with the polymer solution. The numerical mass transfer model coupled chemical reactions and mass and heat transfer phenomena and it did not contain any adjustable parameter. The model was validated using experimental data collected in-line, by following the progression of the gelation front from the top to the bottom of the sample. The agreement between the model predictions and a various sets of experimental data exhibited that the model performs adequately well, meaning that the main elementary mechanisms involved in the gelation were described fairly well. The experimental and numerical results showed that the gelation rate was very similar whatever the process (wet or vapor gelation processes) once the initial driving force for ammonia transfer is the same (the ammonia chemical potential in the bulk phase). Moreover, it was pointed out that the main resistance to transfer was located in the chitosan solution even if an increase of the external mass transfer coefficient can affect the whole gelation time for smooth external conditions (free convection or low flow rate in vapor phase or low stirring speed in wet process). The degree of acetylation slightly influenced the gelation rate because the DA controls the number of amino groups on chitosan chains. Besides, the gelation process was influenced by the temperature because the gelation was mainly governed by diffusion mechanisms. Significant decreases of the gelation time were observed when increasing the temperature of the fabrication chamber. The influence of the external hydrodynamic conditions for both processes was investigated by the numerical model. For each process, the model predictions exhibited that increasing the external mass transfer rate by imposing a stirring (wet process) or an air flow (vapor gelation process) allowed decreasing the gelation time. However, above a critical value, keeping on increasing the external transfer rate did not affect the mass transfer resistance no more, which was located into the bulk phase. Finally, the numerical model demonstrated that the heat transfer should be coupled to the mass transfer in the vapor process model since heat consumption or production could affect the external transfer rate. At last, with regards to the low sample thickness and the operating conditions used in this work, very weak temperature gradients were obtained in the sample thickness.

Acknowledgments

The authors thank the French National Agency of Research (ANR) which supported this study through the project PANSKIT (ANR-08-MAPR-0021-01).

Notation

a_a = activity of ammonia
a_w = activity of water
c_i = concentration of i (mol/m^3)
Ca = capillary number
Cp_{chit} = heat capacity of the polymeric solution (J/kg K)
Cp_g = heat capacity of glass (J/kg K)
Cp_{ss} = heat capacity of inox (J/kg K)
Cp_w = heat capacity of water (J/kg K)
$D_{i/g}$ = mutual diffusion coefficient of i in the gas phase (m^2/s)
$D_{i/m}$ = mutual diffusion coefficient of i within the matrix (m^2/s)
g = acceleration due to gravity (m/s^2)
Gr = Grashof number
h = heat transfer coefficient (W/m^2 K)
h_a = heat transfer coefficient at the interface between the ammonia solution and the polymeric system (W/m^2 K)
h^{up} = heat transfer coefficient at the air side (W/m^2 K)
h^{down} = heat transfer coefficient at the bottom of the system (W/m^2 K)
H_g = glass graduated measuring tube thickness (m)
H_{chit} = polymeric system thickness (m)
H_S = position of the upper interface (m)
H_{ss} = stainless steel plate thikness (m)
ΔH_R = enthalpy of reaction between acetic acid and ammonia (J/kg)
ΔH_{vi} = heat of vaporization of i (J/kg)
i = current intensity (A)
J_i = mass flux of i (kg/m^2 s)
J_{i/amm_sol} = mass flux of i in the ammonia solution (kg/m^2 s)
k_i = mass transfer coefficient of i for free convection (s/m)
k_i = mass transfer coefficient of i at the liquid/liquid interface, in stirring conditions (m/s)
k_j^f = forward kinetic constant (L/mol s)
k_j^r = reverse kinetic constant (L/mol s)
L_c = characteristic length of the interface (m)
M_i = molecular mass of i (kg/mol)
Pr = Prandtl number
pK_{a1} = negative logarithm of the dissociation constant of the NH_4^+/NH_3 couple
pK_{a2} = negative logarithm of the dissociation constant of the Chit-NH_3^+/Chit-NH_2 couple
pK_{a3} = negative logarithm of the dissociation constant of the AcOH/AcO^- couple
P_{svi} = saturating vapor pressure of i (Pa)
P_{vi} = vapor pressure of i (Pa)
Q = heat generation or consumption term (W/m^3)
R = resistance used to heat the solution within the calorimeter (Ω)
R_i = rate expression for a given specie i (mol/L s)
Re = Reynolds number
Re' = modified Reynolds number
RH = relative humidity in the atmosphere in the reactor (%)
Sc_i = Schmidt number
Sh = Sherwood number
T_b = temperature of the bulk (K)
T_f = final temperature inside the calorimeter (K)
T_i = initial temperature inside the calorimeter (K)
T_{sample} = temperature of the sample (K)
V_1 = molar volume of ammonia (cm^3/mol)
$y_{air,lm}$ = log mean mole fraction difference of air
H = dimensionless position
λ_a = thermal conductivity of air (W/m K)
λ_g = thermal conductivity of glass (W/m K)

λ_{ss} = thermal conductivity of inox (W/m K)
Λ_2 = thermal conductivity of water (W/m K)
ν_{NS} = kinematic viscosity of the ammonia solution (m^2/s)
ν_{sol} = kinematic viscosity of the chitosan solution (m^2/s)
μ_2 = viscosity of water (cP)
ρ_a = air density (kg/m^3)
ρ_g = density of the glass Petri dish (kg/m^3)
ρ_s = density of the solution (kg/m^3)
ρ_{ss} = density of the stainless steal plate (kg/m^3)
$\rho_i(t)$ = local concentration of i (kg/m^3)
ρ_{i0}^{η} = initial concentration of i (kg/m^3)
ρ_{i0}^{e} = concentration of i in the gas phase (kg/m^3)
ρ_i^t = concentration of i at the interface (kg/m^3)
φ = correction factor
ϕ = association factor of water
AcOH = acetic acid
AcO^- = acetate ion
Chit-NH_3^+ = chitosan under soluble form
Chit-NH_2 = chtiosan under gel form
NH_3 = Ammonia
NH_4^+ = ammonium ion
OH^- = hydroxide ion
VIPS = vapor induced phase separation

Literature Cited

1. Vachoud L, Domard A. Physicochemical properties of physical chitin hydrogels: modeling and relation with the mechanical properties. *Biomacromol*. 2001;2:1294–1300.
2. Ravindra R, Krovvidi KR, Khan AA. Solubility parameter of chitin and chitosan. *Carbohydr Polym*. 1998;36:121–127.
3. Mi FL., Shyu SS, Wu YB, Lee ST, Shyong JY, Huang RN. Fabrication and characterization of a sponge-like asymmetric chitosan membrane as a wound dressing. *Biomaterials*. 2001;22:165–173.
4. Adekogbe I, Ghanem A. Fabrication and characterization of DTBP-crosslinked chitosan scaffolds for skin tissue engineering. *Biomaterials*. 2005;26:7241–7250.
5. Mi FL, Wu YB, Shyu SS, Chao AC, Lai JY, Su CC. Asymmetric chitosan membranes prepared by dry/wet phase separation: a new type of wound dressing for controlled antibacterial release. *J Membr Sci*. 2003;212:237–254.
6. Hong Y, Song H, Gong Y, Mao Z, Gao C, Shen J. Covalently crosslinked chitosan hydrogel: properties of in vitro degradation and chondrocytes encapsulation. *Acta Biomater*. 2007;3:23–31.
7. Venault A, Vachoud L, Pochat C, Bouyer D, Faur C. Elaboration of chitosan-activated carbon composites for the removal of organic micropollutants from waters. *Environ Technol*. 2008;29:1285–1296.
8. Park HC, Kim YP, Kim HY, Kang YS. Membrane formation by water vapor induced phase inversion. *J Membr Sci*. 1999;156:169–172.
9. Menut P, Pochat-Bohatier C, Deratani A, Dupuy C, Guilbert S. Structure formation of poly(ether-imide) films using non-solvent vapor induced phase separation: relationship between mass transfer and relative humidity. *Desalination*. 2002;145:11–16.
10. Ripoche A, Menut P, Dupuy C, Caquineau H, Deratani A. Poly (ether imide) membrane formation by water vapour induced phase separation. *Macromol Symp*. 2002;188:37–48.
11. Chinpa W, Bouyer D, Pochat-Bohatier C, Deratani A, Dupuy C. Effect of a drying pretreatment on morphology of porous poly(ether-imide) membrane prepared using vapor-induced phase separation. *Dry Technol*. 2006;24:1317–1326.
12. Montembault A, Viton C, Domard A. Rheometric study of the gelation of chitosan in aqueous solution without cross-linking agent. *Biomacromol*. 2005;6:653–662.
13. Vachoud L, Zydowicz N, Domard A. Formation and characterization of a physical chitin gel. *Carbohydr Res*. 1997;302:169–177.
14. Venault A, Bouyer D, Pochat C, Vachoud L, Faur C. Modeling the mass transfers during the elaboration of chitosan-activated carbon composites for medical applications. *AIChE J*. 2010;56:1593–1609.
15. Bouyer D, Vachoud L, Chakrabandhu Y, Pochat-Bohatier C. Influence of mass transfer on gelation time using VIPS-gelation process for chitin dissolved in LiCl/NMP solvent—modeling and experimental study. *Chem Eng J*. 2010;157:605–619.
16. Chakrabandhu Y. Process influence on chitin hydrogel elaboration by non-solvent induced gelation, PhD thesis, University of Montpellier II, 2009.
17. Venault A., Elaboration of chitosan/activated carbon composites hydrogels for wound dressing applications by phase inversion processes, PhD thesis, University of Montpellier II, 2010.
18. Cheng LP, Lin DJ, Shih CH, Dwan AH, Gryte CC. PVDF membrane formation by diffusion-induced phase separation-Morphology prediction based on phase behaviour and mass transfer modeling. *J Polym Sci B: Polym Phys*. 1999;37:2079–2092.
19. Fernandes GR, Pinto JC, Nobrega R. Modeling and simulation of the phase-inversion process during membrane preparation. *J Appl Polym Sci*. 2001;82:3036–3051.
20. Kim YD, Kim JY, Lee HK, Kim SC. A new modeling of asymmetric membrane formation in rapid mass transfer system. *J Membr Sci*. 2001;190:69–77.
21. Matsuyama H, Teramoto M, Nakatani R, Maki T. Membrane formation via phase separation induced by penetration of nonsolvent from vapor phase. I. Phase diagram and mass transfer process. *J Appl Polym Sci*. 1999;74:159–170.
22. Khare VP, Greenberg AR, Krantz WB. Vapor-induced phase separation-effect of the humid air exposure step on membrane morphology Part I. Insights from mathematical modeling. *J Membr Sci*. 2005;258:140–156.
23. Yip Y, McHugh AJ. Modeling and simulation of nonsolvent vapor-induced phase separation. *J Membr Sci*. 2006;271:163–176.
24. Bouyer D, Werapun W, Pochat-Bohatier C, Deratani A. Morphological properties of membranes fabricated by VIPS process using PEI/NMP/water system: SEM analysis and mass transfer modeling. *J Membr Sci*. 2010;349:97–112.
25. Perry RH, Green DW. *Perry's Chemical Engineers' Handbook*, 6th ed. New York: McGraw-Hill, 1984.
26. Shojaie SS, Krantz WB, Greenberg AR. Dense polymer film and membrane formation via the dry-cast process. Part I. Model development. *J Membr Sci*. 1994;94:255–280.
27. Alsoy S, Duda JL. Modeling of multicomponent drying of polymer films. *AIChE J*. 1999;45:896–905.
28. Zielinski JM, Duda JL. Predicting polymer/solvent diffusion coefficients using free-volume theory. *AIChE J*. 1992;38:405–415.
29. Wilke CR, Chang P. Correlation of diffusion coefficients in dilute solutions. *AIChE J*. 1955;1:264–270.
30. Asai S, Hatanaka J, Uekawa Y. Liquid-liquid mass transfer in an agitated vessel with a flat interface. *J Chem Eng Jpn*. 1983;16:463–469.
31. Welty JR, Wicks CE, Wilson RE. *Fundamentals of Momentum, Heat, and Mass Transfer*, 3rd ed. New York: Wiley, 1984.
32. Roustan M. *Transferts gaz-liquide dans les procedes de traitement des eaux et des effluents gazeux*. Paris, France: Ed. Tec & Doc, 2003.
33. Eigen M, De Maeyer L. Rate of neutralization reaction. *Naturwissenschaften*. 1955;42:413–414.
34. Gutman M, Nachliel E, Gherson E, Giniger R. Kinetic analysis of the protonation of a surface group of a macromolecule. *Eur J Biochem*. 1983;134:63–69.
35. Vachoud L. Etude de la relation structure-propriétés des gels de chitine, PhD thesis, University of Lyon I, 1999.
36. McHugh AJ, Miller DC. The dynamic of diffusion and gel growth during nonsolvent-induced phase inversion of polyethersulfone. *J Membr Sci*. 1995;105:121–136.
37. Qin PY, Chen CX, Yun YB, Chen Z, Shintani T, Li X, Li JD, Sun BH. Formation kinetics of polyphthalazine ether sulfone ketone membrane via phase inversion. *Desalination*. 2006;186:229–237.
38. Qin PY, Chen CX, Han B, Takuji S, Li J, Sun B. Preparation of poly(phthalazinone ether sulfone ketone) asymmetric ultrafiltration membrane II. The gelation process. *J Membr Sci*. 2006;268:181–188.
39. Kaiser V, Stropnik C, Musil V, Brumen B. Morphology of solidified polysulfone structures obtained by wet phase separation. *Eur Polym J*. 2007;43:2515–2524.
40. Yi Z, Zhu LP, Xu YY, Zhao YF, Ma XT, Zhu BK. Polysulfone-base amphiphilic polymer for hydrophilicity and fouling-resistant modification of polyethersulfone membranes. *J Membr Sci*. 2010;365:25–33.
41. Tsai HA, Kuo CY, Lin JH, Wang DM, Deratani A, Pochat-Bohatier C, Lee KR, Lai JY. Morphology control of polysulfone hollow fiber membranes via water vapor induced phase separation. *J Membr Sci*. 2006;278:390–400.
42. Liu QL, Gao HQ. Prediction of mutual-diffusion coefficients in polymer solutions using a simple activity coefficient model. *J Membr Sci*. 2003;2414:131–142.

43. Reis RA, Nobrega R, Oliveira JV, Tavares FW. Self- and mutual diffusion coefficient equation for pure fluids, liquid mixtures and polymeric solutions. *Chem Eng Sci*. 2005;60:4581–4592.
44. Tonge MP, Stubbs JM, Sundberg DC, Gilbert RG. Penetrant diffusion in poly(methyl methacrylate) near T_g: dependence on temperature and polymer weight fraction. *Polymer*. 2000;41:3659–3670.
45. Chenite A, Gori S, Shive M, Desrosiers E, Buschmann MD. Monolithic gelation of chitosan solutions via enzymatic hydrolysis of urea. *Carbohydr Polym*. 2006;64:419–424.
46. Hwang KT, Kim JT, Jung ST, Cho GS, Park HJ. Properties of chitosan-based biopolymer films with various degrees of deacetylation and molecular weights. *J Appl Polym Sci*. 2003;89:3476–3484.
47. Minagawa T, Okamura Y, Shigemasa Y, Minami S, Okamoto Y. Effects of molecular weight and deacetylation degree of chitin/chitosan on wound healing. *Carbohydr Polym* 2007;67:640–644.

Appendix A: Calorimetric Measurements: Numerical Data

• At first, the heat capacity of the calorimeter was determined. $w_e = 50 \times 10^{-3}$ kg of distilled water were poured in the calorimeter immersed in the bath of distilled water heated up at 303 ± 0.1 K. Then, the inside of the calorimeter was heated thanks to small electrodes penetrating within the solution. The heat capacity of the whole system-calorimeter and water-C_t (J/K) was calculated thanks to Eq. A1

$$Q = r \times i^2 \times t = -\mathrm{Cp_t} \times (T_\mathrm{f} - T_i) = -(\mathrm{Cp_c} + \mathrm{w_e Cp_w}) \times (T_\mathrm{f} - T_i) \tag{A1}$$

where Q (J) is the total heat exchanged, r (Ω) the resistance of the electrode, i (A) the current intensity, $\mathrm{Cp_t}$ (J/K), the total heat capacity, t (s) the time, T_f and T_i (K), the final and initial temperatures, respectively. $\mathrm{Cp_w}$ (J/K kg) is the heat capacity of water and $\mathrm{Cp_c}$ (J/K), the heat capacity of the calorimeter. After several measurements, the mean value of $\mathrm{Cp_c}$ was found to be 89.22 J/K.

• The second step was dedicated to the determination of the enthalpy of reaction between acetic acid and ammonia ΔH_R (J/mol). To allow a total solubilization of chitosan, a slight excess (5%) of acetic acid was added. Ammonia first reacts with this excess before inducing chitosan gelation. To estimate ΔH_R, 0.59 ml of acetic acid 80% wt were added to 50 g of distilled water. It corresponded to the amount of acid necessary to prepare 50 g of a 3.5% w/v chitosan solution. No temperature variation was recorded when acid was added to water. Then, 0.67 ml of ammonia 28% wt was added to the mixture. In this case, temperature increased from 302.53 to 304.08 K and it was possible to calculate the global heat exchanged using Eq. A2

$$Q = -\mathrm{Cp_t} \times \Delta T = n \times \Delta H_\mathrm{R} \tag{A2}$$

where ΔT (K) is the temperature variation measured and n (mol) the amount of acid. Finally, ΔH_R was measured to be: 55968.1 J/mol. It was also verified that adding ammonia in excess did not lead to a temperature change. Hence, the heat of dilution of ammonia in the present system is 0 J.

• The next step concerned the experimental determination of the heat capacity of a chitosan solution (Batch 342) $\mathrm{Cp_{chit}}$ (J/K). To do it, the same procedure as the one used to estimate the heat capacity of the calorimeter was used. But in this case, water was replaced by 50 g of a 3.5% w/v chitosan solution. The choice of the concentration is related to the fact that below 3%, final gels are too smooth to be used, and above 4%, polymeric solutions are too viscous to be homogeneously casted. In that experiment, ΔT was measured to be 2.1 K. Replacing $\mathrm{Cp_w}$ by $\mathrm{Cp_{chit}}$ in Eq. A1 leads to C_chit = 4650 J/K kg which is rather closed to the heat capacity of distilled water ($\mathrm{Cp_w}$ = 4184 J/K kg).

• Finally, the heat of gelation, ΔH_gel (J/mol) was measured. The necessary amount of ammonia was added to 50 g of a 3.5% w/v chitosan solution. Injection of ammonia had to be quick to permit the homogenization of the mixture before gelling, and stirring had to be fast. As no temperature change was recorded, ΔH_gel was 0 J/mol. Therefore, it was assumed that if heat was created during the neutralization of chitosan chains by ammonia, it was balanced by the reorganization of polymeric chains occurring during gelation.

Manuscript received Feb. 11, 2011, and revision received Jun. 22, 2011.